Functional Role of TRPV4-$K_{Ca}2.3$ Signaling in Vascular Endothelial Cells in Normal and Streptozotocin-Induced Diabetic Rats

Xin Ma, Juan Du, Peng Zhang, Jianxin Deng, Jie Liu, Francis Fu-Yuen Lam, Ronald A. Li, Yu Huang, Jian Jin and Xiaoqiang Yao

Hypertension. 2013;62:134-139; originally published online May 6, 2013;
doi: 10.1161/HYPERTENSIONAHA.113.01500
Hypertension is published by the American Heart Association, 7272 Greenville Avenue, Dallas, TX 75231

Print ISSN: 0194-911X. Online ISSN: 1524-4563

Functional Role of TRPV4-K_{Ca}2.3 Signaling in Vascular Endothelial Cells in Normal and Streptozotocin-Induced Diabetic Rats

Xin Ma,* Juan Du,* Peng Zhang, Jianxin Deng, Jie Liu, Francis Fu-Yuen Lam, Ronald A. Li, Yu Huang, Jian Jin, Xiaoqiang Yao

Abstract—The small conductance and intermediate conductance Ca^{2+}-activated K^+ channels are known to be involved in the endothelium-dependent hyperpolarization. Ca^{2+} entry into endothelial cells stimulates these channels, causing membrane hyperpolarization in endothelial cells and underlying smooth muscle cells. In the present study, with the use of coimmunoprecipitation and double immunolabeling methods, we demonstrated a physical interaction of transient receptor potential vanilloid 4 (TRPV4) with K_{Ca}2.3 in rat mesenteric artery endothelial cells. Acetylcholine and 4α-PDD mainly acted through TRPV4-K_{Ca}2.3 pathway to induce smooth muscle hyperpolarization and vascular relaxation. K_{Ca}3.1 was also involved in the process but at a much lesser degree than that of K_{Ca}2.3. Stimulating TRPV4-K_{Ca}2.3 signaling pathway also increased local blood flow in mesenteric beds and reduced systemic blood pressure in anesthetized rats. In streptozotocin-induced diabetic rats, the expression levels of TRPV4 and K_{Ca}2.3 were reduced, which could be an underlying reason for the dysfunction of endothelium-dependent hyperpolarization in these animals. These results demonstrated an important physiological and pathological role of TRPV4-K_{Ca}2.3 signaling pathway in vascular endothelial cells. (***Hypertension*. 2013;62:134-139.**) ● **Online Data Supplement**

Key Words: endothelial cells ■ endothelium-derived hyperpolarizing factor ■ TRPV4-K_{Ca}2.3 association ■ vascular relaxation

Vasoactive agonists, including acetylcholine and bradykinin, induce vascular dilation by stimulating endothelial cells to release NO and prostacyclin and by mechanisms involving endothelium-derived hyperpolarizing factors (EDHFs). One of the most important EDHF mechanisms involves 2 populations of endothelial cell K^+ channels, the small conductance and intermediate conductance Ca^{2+}-activated K^+ channels (SK_{Ca} and IK_{Ca}), respectively.[1–4] There are 3 SK_{Ca} isoforms, but only K_{Ca}2.3 is known to be important for EDHF responses.[5] Activity of K_{Ca}2.3 and IK_{Ca} (K_{Ca}3.1) not only directly hyperpolarizes vascular endothelial cells but also indirectly hyperpolarizes the underlying vascular smooth muscle cells via multiple mechanisms.[1,2] This K_{Ca}2.3- or K_{Ca}3.1-mediated EDHF mechanism exists in a wide variety of vascular beds, participating in the control of local blood perfusion and overall body blood pressure.[1,2]

A key early event in the K_{Ca}2.3- or K_{Ca}3.1-mediated EDHF responses is the rise of cytosolic Ca^{2+} ($[Ca]^{2+}_i$) in endothelial cells.[1,2] The $[Ca]^{2+}_i$ rises then activate K_{Ca}2.3 and K_{Ca}3.1.[1,2] Recent studies have suggested a causal link between several Ca^{2+}-permeable transient receptor potential channels (transient receptor potential vanilloid [TRVP] 4, TRPA1, TRPV3, and TRPC6) and K_{Ca} channels (K_{Ca}2.3 and K_{Ca}3.1) in endothelial cells.[6–13] Presumably, the Ca^{2+} entry through these TRP channels would activate either K_{Ca}2.3 or K_{Ca}3.1. However, still there is lack of evidence for specific interaction of any TRP isoform (TRPV4 or TRPA1 or TRPV3 or TRPC6) with a K_{Ca} channel (either K_{Ca}2.3 or K_{Ca}3.1) in endothelial cells. Our previous study showed that TRPC1 is physically associated with another K_{Ca} channel (K_{Ca}1.1 or BK_{Ca}) in vascular smooth muscle cells.[14] Such type of physical interaction would allow more efficient signal transduction between 2 molecules.[14] It will be interesting to find out whether similar physical interaction exists between a TRP channel and an endothelial cell K_{Ca} channel.

EDHF-mediated responses are clearly altered in various pathological conditions.[15] In the pathogenesis of hypertension and diabetes mellitus, vascular relaxant actions of NO and EDHFs are both impaired, contributing to disease progression.[15] However, in some other pathological conditions, including congestive heart failure, hypercholesterolemia, ischemia-reperfusion, and restenosis after coronary angioplasty, the NO-mediated relaxant response is impaired, whereas the EDHF-mediated relaxant response is increased as a compensation.[15]

Received April 2, 2013; first decision April 2, 2013; revision accepted April 14, 2013.

From the School of Medicine and Pharmaceutics, Jiangnan University, Wuxi, China (X.M., J.J., X.Y.); School of Biomedical Sciences (X.M., J.D., P.Z., F.F.-Y.L., Y.H., X.Y.) and Shenzhen Research Institute (P.Z., X.Y.), Chinese University of Hong Kong, Hong Kong, China; Department of Physiology, Anhui Medical University, Hefei, China (J.D., X.Y.); Department of Pathophysiology, Southern Medical University, Guangzhou, China (J.De.); Department of Pathophysiology, Shenzhen University, Shenzhen, China (J.L.); and Stem Cell and Regenerative Medicine Consortium, University of Hong Kong, Hong Kong, China (R.A.L.).

*X. Ma and J. Du contributed equally to this article.

The online-only Data Supplement is available with this article at http://hyper.ahajournals.org/lookup/suppl/doi:10.1161/HYPERTENSIONAHA.113.01500/-/DC1.

Correspondence to Xiaoqiang Yao, School of Biomedical Sciences, The Chinese University of Hong Kong, Hong Kong, China. E-mail yao2068@cuhk.edu.hk

Hypertension **is available at http://hyper.ahajournals.org** **DOI: 10.1161/HYPERTENSIONAHA.113.01500**

However, the molecular mechanism of altered EDHF responses in these disease states is poorly understood.

In the present study, we identified a previously unknown physical association between TRPV4 and K_{Ca}2.3 and uncovered the functional role of this TRPV4-K_{Ca}2.3 signaling pathway in smooth muscle hyperpolarization and relaxation. We also found that reduced expression levels of TRPV4 and K_{Ca}2.3 could be an underlying mechanism for EDHF dysfunction in diabetic rats.

Materials and Methods

See the Methods section in the online-only Data Supplement for details.

Cell Preparation and Culture

All animal experiments were conducted in accordance with the regulation of the US National Institute of Health (NIH) Guide for the Care and Use of Laboratory Animals. Primary mesenteric artery endothelial cells (MAECs) were isolated from male Sprague-Dawley rats, cultured for 3 to 5 days, and used for experiments without passage.

Immunostaining, Immunoprecipitation, and Immunoblots

Double immunolabeling was performed in rat MAECs using anti-TRPV4 antibody together with either anti-K_{Ca}2.3 or anti-K_{Ca}3.1 antibody. Artery sections were stained with either anti-TRPV4 or anti-K_{Ca}2.3 antibody. Immunoprecipitation and immunoblots were performed following the protocol described elsewhere with slight modifications.[16]

Membrane Potential and $[Ca]^{2+}_i$ Measurement

Fura-2 and $DiBAC_4(3)$ were loaded in rat MAECs for simultaneous measurement of membrane potentials and $[Ca]^{2+}_i$. The membrane potentials of MAECs were also measured using perforated whole-cell patch clamp with an EPC-9 amplifier. High-impedance sharp microelectrodes were used to measure smooth muscle cell membrane potentials in isolated arteries.

Arterial Tension Measurement

Segments of the third or fourth branches of rat mesenteric artery were isolated. The tension was measured using a DMT myograph.

Blood Flow Measurement

Approximately two thirds of rat mesenteric arterial bed was put on a petri dish, and the local blood perfusion was assessed with a Laser Doppler perfusion imager. Body blood pressure was simultaneously monitored through a pressure transducer inserted in common carotid artery.

Induction of Diabetes Mellitus

A single dose of streptozotocin (60 $mg \cdot kg^{-1}$, IP) was injected in rats to induce diabetes mellitus.

Statistics

Paired 2-tailed Student *t* test was used for 2-group comparison. For dose–response curves (Figures 2B, 3C, 3D, 5B, and 5C), acetylcholine concentration was transformed into log values, and the data were fitted with sigmoidal dose–response curves. *F* test was performed to compare the best-fit values of E_{MAX} and EC_{50} between different treatments (GraphPad). $P<0.05$ was considered as significantly different.

Results

Physical and Functional Interaction of TRPV4 and K_{Ca}2.3

In double immunolabeling experiments, K_{Ca}2.3 staining (Alexa fluor 488, green) and TRPV4 staining (Alexa fluor 546, red) were found to have significant distribution in the plasma membrane of the primary cultured rat MAECs (Figure 1A). In merged image, there was strong overlapping of K_{Ca}2.3 and TRPV4 fluorescence (yellow) indicated by high percentage of pixel-to-pixel colocalization (Figure 1A). In control experiments, there was no staining if the primary antibodies were preabsorbed with excessive amounts of respective antigens (data not shown). K_{Ca}3.1 expression was also observed in the plasma membrane, but its colocalization with TRPV4 was much less than that of K_{Ca}2.3 (Figure S1 in the online-only Data Supplement). In coimmunoprecipitation experiments, an anti-K_{Ca}2.3 antibody could pull down TRPV4 proteins in the lysates freshly prepared from rat MAECs (Figure 1B). Furthermore, an anti-TRPV4 antibody could reciprocally pull down K_{Ca}2.3 (Figure 1B). In contrast, the

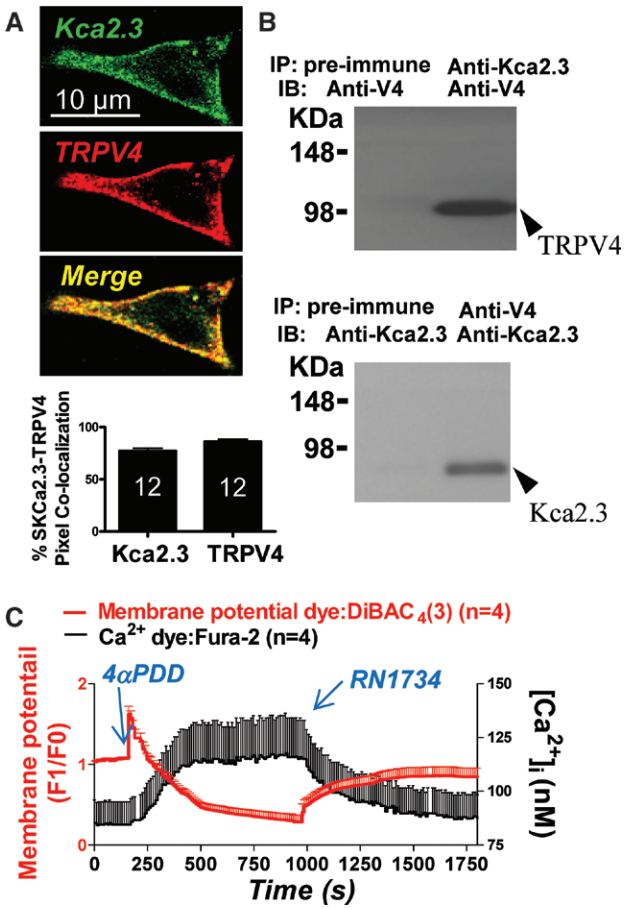

Figure 1. Physical and functional interaction of TRPV4 and K_{Ca}2.3 in the primary cultured rat mesenteric artery endothelial cells (MAECs). **A**, Subcellular colocalization of TRPV4 with K_{Ca}2.3 in the primary cultured rat MAECs. Shown were immunostaining images of K_{Ca}2.3 (green) and TRPV4 (red) in a representative cell; also shown were the overlay image (merge) and data summary illustrating the percentage of TRPV4-K_{Ca}2.3 pixel colocalization (**bottom**). Data are shown as mean±SE (n=12 cells). **B**, Coimmunoprecipitation of TRPV4 with K_{Ca}2.3 in the primary cultured rat MAECs. The pulling antibody and blotting antibody were indicated. Control immunoprecipitation was done using preimmune IgG (preimmune). Anti-V4 indicates anti-TRPV4; IB, immunoblot; and IP, immunoprecipitation. n=4 experiments. **C**, Simultaneous measurement of membrane potentials and $[Ca]^{2+}_i$ in rat MAECs using fluorescence dyes Fura-2/AM and $DiBAC_4(3)$. 4α-PDD (5 μmol/L) and RN-1734 (10 μmol/L) were applied to the bath at the time indicated by arrows, n=4.

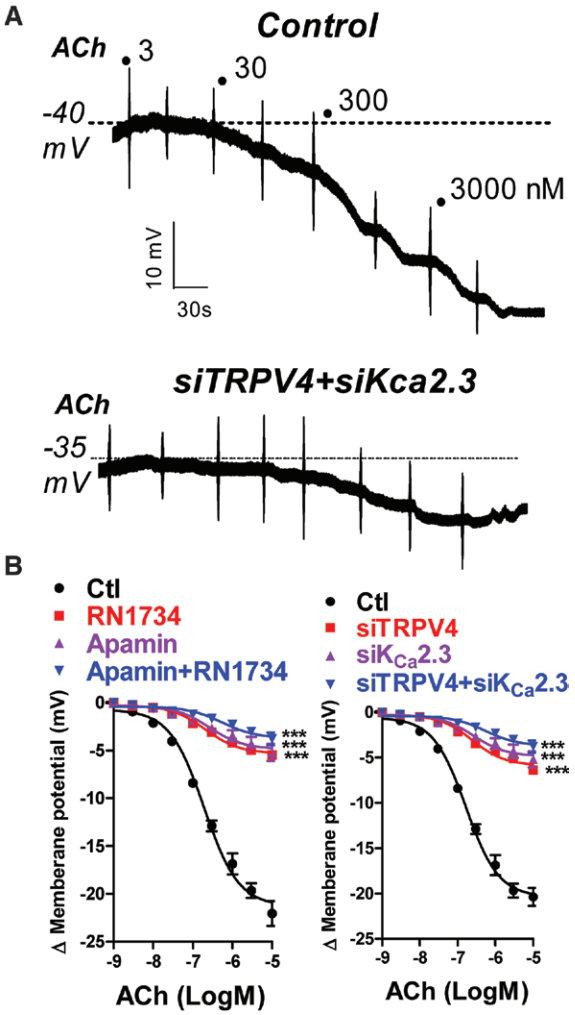

Figure 2. Sharp microelectrode measurement of smooth muscle cell membrane potentials in isolated mesenteric arteries. **A**, Representative traces of sharp microelectrode measurement of smooth muscle membrane potentials in isolated mesenteric artery strips. Shown are dose-dependent hyperpolarization to acetylcholine (ACh; 3 nmol/L–10 μmol/L) and the effect of TRPV4-siRNA plus K_{Ca}2.3-siRNA. **B**, Summary data showing the effect of TRPV4 or K_{Ca}2.3 inhibition/suppression on ACh-induced hyperpolarization. If needed, the artery strips were pretreated with RN-1734 (10 μmol/L), apamin (200 nmol/L), or RN-1734 plus apamin for 30 minutes. Data in mean±SE were fitted with sigmoidal dose–response curve. *F* test was used to compare the best-fit values of E_{MAX} and EC_{50} between different groups. n=4 to 8 experiments. ***P<0.001 compared with control (Ctl) for both E_{MAX} and EC_{50}.

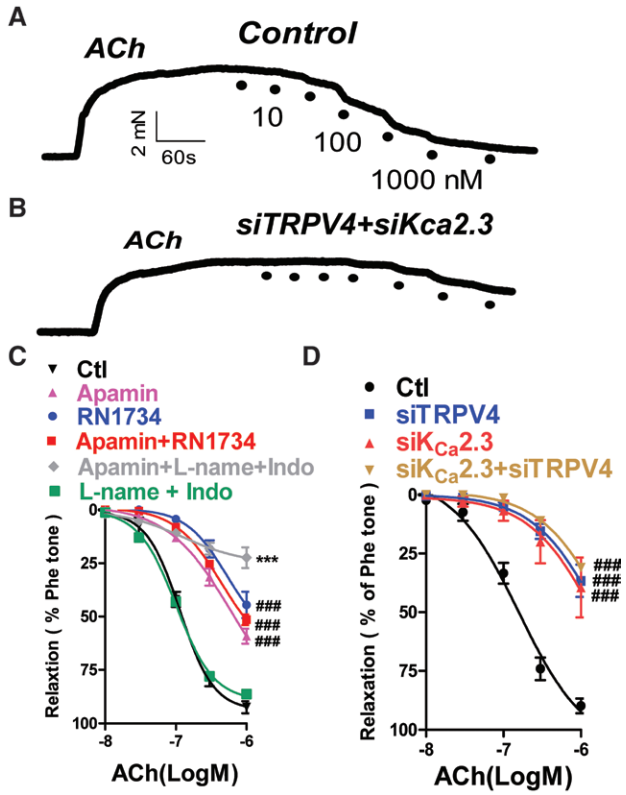

Figure 3. Role of TRPV4-K_{Ca}2.3 pathway in acetylcholine-induced vascular relaxation. **A** and **B**, Representative traces of acetylcholine-induced vascular relaxation. Shown were dose-dependent relaxation to acetylcholine (ACh; 0.01–1 μmol/L) and the effect of TRPV4-siRNA plus K_{Ca}2.3-siRNA. **C** and **D**, Summary data of myograph studies showing the effect of TRPV4 or K_{Ca}2.3 inhibition/suppression on ACh-induced relaxation. If needed, the arterial segments were pretreated with RN-1734 (10 μmol/L), apamin (200 nmol/L), apamin plus L-NAME (100 μmol/L) plus indomethacin (10 μmol/L), or L-NAME (100 μmol/L) plus indomethacin (10 μmol/L) for 30 minutes. Data in mean±SE were fitted with sigmoidal dose–response curve. *F* test was used to compare the best-fit values of E_{MAX} and EC_{50} between different groups. n=4 to 8 experiments. ###P<0.001 compared with control for EC_{50}. ***P<0.001 compared with RN-1734 or apamin or RN-1734 plus apamin for both E_{MAX} and EC_{50}.

anti-TRPV4 antibody failed to pull down K_{Ca}3.1 and vice versa (Figure S1). These data indicate that TRPV4 physically associates with K_{Ca}2.3 but not with K_{Ca}3.1.

Ca^{2+}-sensitive and membrane potential–sensitive fluorescence dyes, Fura-2/AM and $DiBAC_4(3)$, were used to simultaneously record the changes of $[Ca]^{2+}_i$ and membrane potentials in rat MAECs. 4α-PDD (5 μmol/L) elicited a biphasic change in membrane potentials, a sudden membrane depolarization followed by a slow hyperpolarization (Figure 1C). The time course of hyperpolarization matched well with that of 4α-PDD–induced $[Ca]^{2+}_i$ rises (Figure 1C). RN-1734 (10 μmol/L, a highly selective TRPV4 antagonist) inhibited both the hyperpolarization and $[Ca]^{2+}_i$ rises, confirming the involvement of TRPV4 in both processes (Figure 1C). 4α-PDD also induced local $[Ca]^{2+}_i$ rises in rat MAECs (Figure S2), similar to the Ca^{2+} sparklets reported elsewhere.[10]

In perforated whole-cell current clamp experiments, 4α-PDD (5 μmol/L) and acetylcholine (1 μmol/L) elicited similar biphasic changes in membrane potentials in rat MAECs (Figure S3). RN-1734 (10 μmol/L) and TRPV4-siRNA substantially inhibited both phases of membrane potential changes (Figure S3). In contrast, apamin (200 nmol/L) and K_{Ca}2.3-siRNA diminished only the hyperpolarization but had no effect on the depolarization (Figure S3). TRAM34 (1 μmol/L, a K_{Ca}3.1 inhibitor) slightly inhibited only the hyperpolarization by ≈20% (Figure S1). For verification, TRPV4-siRNA and K_{Ca}2.3-siRNA could effectively knockdown the expression level of their targeted proteins (Figure S4). Furthermore, K_{Ca}2.3-siRNA did not affect the 4α-PDD–induced $[Ca]^{2+}_i$ rise (Figure S5). These data suggest that, although the depolarization was attributable to TRPV4, the hyperpolarization required the activity of both TRPV4 and K_{Ca}2.3 (and to a less degree of K_{Ca}3.1).

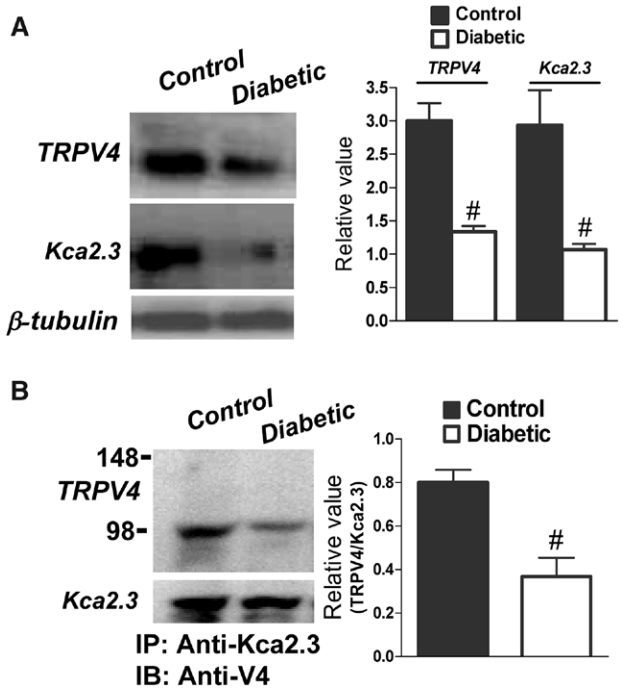

Figure 4. Reduced expression of TRPV4 and K_{Ca}2.3 proteins in diabetic rats. **A**, Western blots comparing the expression of TRPV4 with K_{Ca}2.3 protein levels between the primary cultured mesenteric artery endothelial cells (MAECs) from normal (control) and diabetic rats. **B**, Coimmunoprecipitation experiments comparing the amount of TRPV4-K_{Ca}2.3 complex in the primary cultured MAECs derived from normal and diabetic rats. The pulling antibody and blotting antibody were indicated. Shown are representative immunoblots (**left**) and data summary (**right**). Anti-V4 indicates anti-TRPV4; IB, immunoblot; and IP, immunoprecipitation. Data are shown as mean±SE. n=4 experiments. Paired 2-tailed Student *t* test was used to compare the difference between 2 groups. #P<0.05 compared with control.

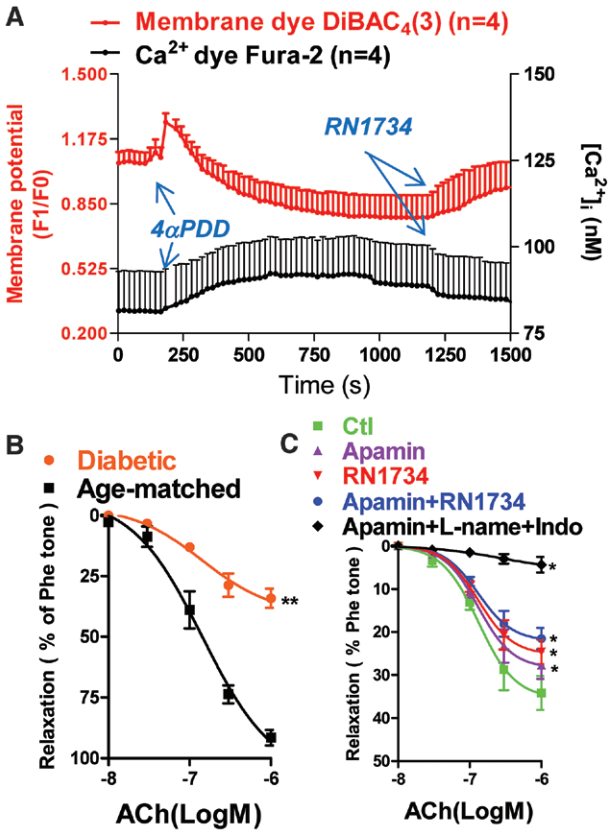

Figure 5. Impaired TRPV4-K_{Ca}2.3 signaling pathway in diabetic rats. **A**, Simultaneous measurement of membrane potentials and $[Ca]^{2+}_i$ in mesenteric artery endothelial cells from diabetic rats using fluorescence dyes. 4α-PDD (5 μmol/L) and RN-1734 (10 μmol/L) were applied to the bath at the time indicated by dotted lines, n=4. **B**, Vascular tension measurement comparing the acetylcholine (ACh)-induced relaxation in the small mesenteric artery segments from age-matched normal and diabetic rats. **C**, Effect of a panel of different inhibitors on acetylcholine-induced relaxation in the small mesenteric artery segments from diabetic rats. Data in mean±SE were fitted with sigmoidal dose–response curve. *F* test was used to compare the best-fit values of E_{MAX} and EC_{50} between different treatments. n=4 to 8 experiments. **P<0.01 compared with diabetic for both E_{MAX} and EC_{50} (**B**). *P<0.05 compared with control (**C**) for both E_{MAX} and EC_{50}.

Role of TRPV4-K_{Ca}2.3 Signaling Axis in 4α-PDD– and Acetylcholine-Induced Smooth Muscle Hyperpolarization and Vascular Relaxation

Immunostaining demonstrated abundant presence of TRPV4 and K_{Ca}2.3 proteins in the endothelium layer in rat mesenteric artery sections (Figure S6). The staining signals were much weaker in the samples prepared from TRPV4-siRNA– or K_{Ca}2.3-siRNA–treated rats (Figure S6).

The membrane potentials of smooth muscle cells were measured in endothelium-intact rat small mesenteric artery strips using high-impedance sharp microelectrodes impaled from adventitial side. Acetylcholine and 4α-PDD each induced smooth muscle hyperpolarization in a concentration-dependent manner (Figure 2; Figure S7). The hyperpolarization was inhibited by RN-1734 (10 μmol/L), TRPV4-siRNA, apamin (200 nmol/L), or K_{Ca}2.3-siRNA (Figure 2; Figure S7), suggesting the involvement of TRPV4 and K_{Ca}2.3. The degree of inhibition by all these treatments was similar in the range of 70% to 80% (Figure 2). Similar results were obtained if the microelectrodes were impaled into smooth muscle cells from adventitial side in pressurized arteries (Figure S8).

In wire myograph study, acetylcholine induced vascular relaxation in a concentration-dependent manner in isolated rat small mesenteric artery segments (Figure 3). The relaxation was inhibited by RN-1734 (10 μmol/L), TRPV4-siRNA, apamin (200 nmol/L), or K_{Ca}2.3-siRNA (Figure 3). The degree of inhibition by all these treatments was similar in the range of 40% to 50% (Figure 3). Apamin plus L-NAME (100 μmol/L) plus indomethacin (10 μmol/L) further reduced the acetylcholine-induced relaxation up to ≈80% (Figure 3C). Typical of K_{Ca}2.3/K_{Ca}3.1-mediated EDHF responses,[2] the hyperpolarization to acetylcholine was not affected by a K_{Ca}1.1 inhibitor iberiotoxin (100 nmol/L; Figure S7), and the relaxation was not affected by L-NAME plus indomethacin (Figure 3C).

Note that the antagonists/siRNAs of TRPV4 and K_{Ca}2.3 potently inhibited the acetylcholine-induced smooth muscle hyperpolarization, which correlated with an increase in EC_{50} values in dose–response curves of acetylcholine-induced vascular relaxation (Figures 2 and 3). This is expected because the vascular relaxation to acetylcholine in rat mesenteric arteries is mediated not only by EDHFs but also by NO.

TRPV4-K_{Ca}2.3 Pathway Regulates Arteriolar Blood Flow and Blood Pressure Ex Vivo

In Laser Doppler imaging experiments, application of 4α-PDD or acetylcholine elicited an increased blood perfusion in mesenteric arteries (Figure S9). These agents also caused a transient reduction in systemic blood pressure (Figure S10). The effect of 4α-PDD and acetylcholine on blood flow and blood pressure was inhibited by RN-1734 and apamin (Figures S9 and S10). Inhibitors alone also caused slight reduction in blood flow (Figure S9). These data suggested a critical role of TRPV4-K_{Ca}2.3 signaling axis in the regulation of systemic blood pressure and local blood perfusion in mesenteric arteries.

Impairment of TRPV4-K_{Ca}2.3 Signaling Axis in Diabetic Rats

Rats were treated with streptozotocin to generate an animal model that mimics type 1 diabetes mellitus. Diabetic rats had serum glucose level of 19.5±0.8 mmol/L (n=11) and body weight of 165±2 g (n=12), whereas normal rats had respective values at 4.5±0.2 mmol/L (n=11) and 368±7 g (n=11). Western blot analysis showed that TRPV4 and K_{Ca}2.3 protein expressions were much lower in MAECs from diabetic rats than those from normal rats (Figure 4A). Coimmunoprecipitation experiments found a reduced amount of TRPV4-K_{Ca}2.3 complex in MAECs from diabetic rats, even after K_{Ca}2.3 protein level was titrated to the same quantity in different loading lane (Figure 4B).

Simultaneous fluorescence measurement of $[Ca]^{2+}_i$ and membrane potentials showed that the $[Ca]^{2+}_i$ rises and hyperpolarization to 4α-PDD (5 μmol/L) and acetylcholine (1 μmol/L) were reduced in cells derived from diabetic rats (Figure 5A) than those from normal rats (Figure 1C). In perforated patch clamp experiments, the changes in membrane potentials in response to 4α-PDD, acetylcholine, and ionomycin, both the depolarization and hyperpolarization phase, were much smaller in cells from diabetic rats than those from normal rats (Figure S11).

In vascular tone study, the acetylcholine-induced mesenteric artery relaxation was markedly reduced by 65% in diabetic rats compared with normal rats (Figure 5B). The residual relaxant response in diabetic rats could be inhibited by apamin (200 nmol/L), RN-1734 (10 μmol/L), or apamin plus RN-1734 (200 nmol/L and 10 μmol/L, respectively; Figure 5C). Apamin plus L-NAME plus indomethacin almost abolished the relaxation (Figure 5C). These data suggest that both TRPV4-K_{Ca}2.3- and NO-mediated relaxation were impaired in diabetic rats.

Discussion

The major findings of this study are as follows: (1) Coimmunoprecipitation and subcellular colocalization demonstrated a physical association of TRPV4 with K_{Ca}2.3 in the primary cultured rat MAECs; (2) 4α-PDD and acetylcholine mainly acted through endothelial cell TRPV4-K_{Ca}2.3 signaling pathway to induce smooth muscle cell hyperpolarization and subsequent vascular relaxation; (3) in anesthetized rats, the TRPV4-K_{Ca}2.3 signaling pathway contributed to the regulation of blood flow and blood pressure; (4) in streptozotocin-induced diabetic rats, the expression level of TRPV4 and K_{Ca}2.3 was reduced, resulting in impaired EDHF responses. Together, these data demonstrate an important physiological and pathological role of TRPV4-K_{Ca}2.3 signaling pathway in EDHF responses.

It is well documented that the mechanisms of EDHFs vary depending on the animal species and vascular beds.[1,2] In rat mesenteric arteries, the main EDHF mechanism involves K_{Ca}2.3,[17] whereas in mouse mesenteric arteries both K_{Ca}2.3 and K_{Ca}3.1 contribute significantly to EDHF responses.[18] Recent studies suggested a functional linkage of TRPV4 to either K_{Ca}2.3 or K_{Ca}3.1 in mouse MAECs.[6,10,11] It was found that the TRPV4-mediated local Ca^{2+} entry (sparklets) predominantly stimulates endothelial cell K_{Ca}3.1, causing relaxation of mouse mesenteric arteries.[10,11] However, these early studies did not provide evidence of whether TRPV4 is physically associated with K_{Ca}3.1. In the present study, we identified a physical association of TRPV4 with K_{Ca}2.3 in rat MAECs. A good temporal correlation was observed between TRPV4-mediated $[Ca]^{2+}_i$ rises and membrane hyperpolarization in the primary cultured MAECs (but the correlation was not tested in intact arteries because of technical difficulty). We also found a critical role of TRPV4-K_{Ca}2.3 signaling pathway in acetylcholine-induced smooth muscle hyperpolarization and relaxation of rat mesenteric arteries. K_{Ca}3.1 was also involved, but its contribution was much smaller than that of K_{Ca}2.3. Together, the results from us and others[6,10,11] demonstrated that TRPV4 may be functionally linked to different K_{Ca} channels depending on animal species. In mouse MAECs, TRPV4 is predominantly coupled to K_{Ca}3.1,[10,11] whereas in rat mesenteric artery, TRPV4 is mainly coupled to K_{Ca}2.3. Because TRPV4 inhibition substantially reduced the acetylcholine-induced smooth muscle cell hyperpolarization by ≈70% to 80% (Figure 2), we reasoned that the contribution of other TRP isoforms (TRPV3, TRPA1, or TRPC6) in the EDHF responses, if any, is small.

It was reported long ago that, in the presence of K_{Ca}2.3 and K_{Ca}3.1 inhibitors, agonists could induce endothelium-dependent smooth muscle depolarization, although the underlying mechanism remains unclear.[19,20] In the present studies, stimulation of TRPV4 induced a biphasic change in endothelial cell membrane potentials, with initial depolarization followed by hyperpolarization (Figure 1; Figure S3). Although the hyperpolarization was mainly attributable to TRPV4-K_{Ca}2.3 coupling, the initial depolarization could be assigned to TRPV4-mediated cation influx because it was altered by TRPV4 activation/inhibition (Figure 1; Figure S3). Thus, it is reasonable to speculate that TRPV4 activity might be the underlying mechanism for the reported endothelium-dependent smooth muscle cell depolarization when K_{Ca}2.3 and K_{Ca}3.1 were inhibited.[19,20] However, note that acetylcholine was reported to induce membrane hyperpolarization without initial depolarization in some endothelial cells,[21] which is different from our results. This discrepancy could be related to variations in vascular beds or TRPV4 expression level.

EDHFs participate in the regulation of local blood flow and systemic blood pressure.[1,2] In diabetes mellitus, EDHF-mediated responses are impaired,[15] contributing to diabetic neuropathy and nephropathy.[22,23] However, the underlying mechanism for the impaired EDHF responses in diabetes mellitus is unclear. In the present study, we demonstrated a crucial role of TRPV4-K_{Ca}2.3 signaling pathway in the regulation of local blood flow and systemic blood pressure. Furthermore, Western blots and coimmunoprecipitation showed a reduced expression level of TRPV4 and K_{Ca}2.3, as well as a reduced

TRPV4-K_{Ca}2.3 complex formation, in endothelial cells in streptozotocin-induced diabetic rats. Therefore, we propose that the reduced TRPV4-K_{Ca}2.3 signaling could be an underlying mechanism for the impaired EDHF responses in diabetic rats.

Perspectives

EDHFs regulate vascular tone, blood perfusion, and blood pressure. EDHF mechanisms are impaired in hypertension and diabetes mellitus.[15] Among many EDHF mechanisms, the one involving endothelial cell K_{Ca}2.3 and K_{Ca}3.1 is the most important, regulating vascular tone in a variety of vascular beds.[1,2] In this study, we uncovered the physical and functional coupling of TRPV4 to K_{Ca}2.3 in endothelial cells. This type of physical association may allow Ca^{2+} entry through TRPV4 to stimulate neighboring K_{Ca}2.3 in subcellular microdomains, causing endothelial cell hyperpolarization. In addition, we found an important role of TRPV4-K_{Ca}2.3 signaling pathway in the control of local blood perfusion and blood pressure. A reduced TRPV4-K_{Ca}2.3 signaling may be an underlying reason for the impaired EDHF responses in diabetic rat models. In the future, it would be interesting to investigate the pathological role of impaired TRPV4-K_{Ca}2.3 signaling in human diabetes mellitus.

Sources of Funding

This work was supported by grants from the Hong Kong Research Grant Committee TBRS T13-706/11, CUHK479109, CUHK478710, CUHK478011 to X. Yao; the Fundamental Research Funds for the Central Universities (JUSRP51311A) to X. Ma; the Program for New Century Excellent Talents in University of the Ministry of Education of China (NCET-12-0880) to X. Ma; and China National Science Foundation 31171100 to X. Yao and 81100185 to X. Ma.

Disclosures

None.

References

1. Triggle CR, Samuel SM, Ravishankar S, Marei I, Arunachalam G, Ding H. The endothelium: influencing vascular smooth muscle in many ways. *Can J Physiol Pharmacol*. 2012;90:713–738.
2. Garland CJ, Hiley CR, Dora KA. EDHF: spreading the influence of the endothelium. *Br J Pharmacol*. 2011;164:839–852.
3. Burnham MP, Bychkov R, Félétou M, Richards GR, Vanhoutte PM, Weston AH, Edwards G. Characterization of an apamin-sensitive small-conductance Ca(2+)-activated K(+) channel in porcine coronary artery endothelium: relevance to EDHF. *Br J Pharmacol*. 2002;135:1133–1143.
4. Bychkov R, Burnham MP, Richards GR, Edwards G, Weston AH, Félétou M, Vanhoutte PM. Characterization of a charybdotoxin-sensitive intermediate conductance Ca2+-activated K+ channel in porcine coronary endothelium: relevance to EDHF. *Br J Pharmacol*. 2002;137:1346–1354.
5. Brähler S, Kaistha A, Schmidt VJ, et al. Genetic deficit of SK3 and IK1 channels disrupts the endothelium-derived hyperpolarizing factor vasodilator pathway and causes hypertension. *Circulation*. 2009;119:2323–2332.
6. Earley S, Pauyo T, Drapp R, Tavares MJ, Liedtke W, Brayden JE. TRPV4-dependent dilation of peripheral resistance arteries influences arterial pressure. *Am J Physiol Heart Circ Physiol*. 2009;297:H1096–H1102.
7. Zhang DX, Mendoza SA, Bubolz AH, Mizuno A, Ge ZD, Li R, Warltier DC, Suzuki M, Gutterman DD. Transient receptor potential vanilloid type 4-deficient mice exhibit impaired endothelium-dependent relaxation induced by acetylcholine *in vitro* and in vivo. *Hypertension*. 2009;53:532–538.
8. Earley S, Gonzales AL, Crnich R. Endothelium-dependent cerebral artery dilation mediated by TRPA1 and Ca2+-Activated K+ channels. *Circ Res*. 2009;104:987–994.
9. Earley S, Gonzales AL, Garcia ZI. A dietary agonist of transient receptor potential cation channel V3 elicits endothelium-dependent vasodilation. *Mol Pharmacol*. 2010;77:612–620.
10. Sonkusare SK, Bonev AD, Ledoux J, Liedtke W, Kotlikoff MI, Heppner TJ, Hill-Eubanks DC, Nelson MT. Elementary Ca2+ signals through endothelial TRPV4 channels regulate vascular function. *Science*. 2012;336:597–601.
11. Bagher P, Beleznai T, Kansui Y, Mitchell R, Garland CJ, Dora KA. Low intravascular pressure activates endothelial cell TRPV4 channels, local Ca2+ events, and IKCa channels, reducing arteriolar tone. *Proc Natl Acad Sci U S A*. 2012;109:18174–18179.
12. Köhler R, Heyken WT, Heinau P, Schubert R, Si H, Kacik M, Busch C, Grgic I, Maier T, Hoyer J. Evidence for a functional role of endothelial transient receptor potential V4 in shear stress-induced vasodilatation. *Arterioscler Thromb Vasc Biol*. 2006;26:1495–1502.
13. Fleming I, Rueben A, Popp R, Fisslthaler B, Schrodt S, Sander A, Haendeler J, Falck JR, Morisseau C, Hammock BD, Busse R. Epoxyeicosatrienoic acids regulate Trp channel dependent Ca2+ signaling and hyperpolarization in endothelial cells. *Arterioscler Thromb Vasc Biol*. 2007;27:2612–2618.
14. Kwan HY, Shen B, Ma X, Kwok YC, Huang Y, Man YB, Yu S, Yao X. TRPC1 associates with BK(Ca) channel to form a signal complex in vascular smooth muscle cells. *Circ Res*. 2009;104:670–678.
15. Félétou M, Vanhoutte PM. EDHF: new therapeutic targets? *Pharmacol Res*. 2004;49:565–580.
16. Ma X, Qiu S, Luo J, Ma Y, Ngai CY, Shen B, Wong CO, Huang Y, Yao X. Functional role of vanilloid transient receptor potential 4-canonical transient receptor potential 1 complex in flow-induced Ca2+ influx. *Arterioscler Thromb Vasc Biol*. 2010;30:851–858.
17. Crane GJ, Gallagher N, Dora KA, Garland CJ. Small- and intermediate-conductance calcium-activated K+ channels provide different facets of endothelium-dependent hyperpolarization in rat mesenteric artery. *J Physiol*. 2003;553(pt 1):183–189.
18. Ding H, Kubes P, Triggle C. Potassium- and acetylcholine-induced vasorelaxation in mice lacking endothelial nitric oxide synthase. *Br J Pharmacol*. 2000;129:1194–1200.
19. Coleman HA, Tare M, Parkington HC. K+ currents underlying the action of endothelium-derived hyperpolarizing factor in guinea-pig, rat and human blood vessels. *J Physiol*. 2001;531(pt 2):359–373.
20. Corriu C, Félétou M, Canet E, Vanhoutte PM. Endothelium-derived factors and hyperpolarization of the carotid artery of the guinea-pig. *Br J Pharmacol*. 1996;119:959–964.
21. Busse R, Fichtner H, Lückhoff A, Kohlhardt M. Hyperpolarization and increased free calcium in acetylcholine-stimulated endothelial cells. *Am J Physiol*. 1988;255(4 pt 2):H965–H969.
22. De Vriese AS, Van de Voorde J, Blom HJ, Vanhoutte PM, Verbeke M, Lameire NH. The impaired renal vasodilator response attributed to endothelium-derived hyperpolarizing factor in streptozotocin–induced diabetic rats is restored by 5-methyltetrahydrofolate. *Diabetologia*. 2000;43:1116–1125.
23. Terata K, Coppey LJ, Davidson EP, Dunlap JA, Gutterman DD, Yorek MA. Acetylcholine-induced arteriolar dilation is reduced in streptozotocin-induced diabetic rats with motor nerve dysfunction. *Br J Pharmacol*. 1999;128:837–843.

Novelty and Significance

What Is New?

- The present study identified a novel physical association of K_{Ca}2.3 with TRPV4 in vascular endothelial cells and uncovered the functional role of TRPV4-K_{Ca}2.3 signaling pathway in smooth muscle hyperpolarization and vascular relaxation.

What Is Relevant?

- TRPV4-K_{Ca}2.3 signaling is important for smooth muscle hyperpolarization and relaxation, thus relevant to blood pressure control and hypertension.

Summary

TRPV4 is physically associated with K_{Ca}2.3 in endothelial cells. This association plays a key role in smooth muscle hyperpolarization and relaxation. The TRPV4-K_{Ca}2.3 signaling pathway is impaired in diabetic rats.

Functional role of TRPV4-K_{Ca}2.3 signaling in vascular endothelial cells in normal and streptozotocin-induced diabetic rats

Xin Ma[1,2,#], Juan Du[2,4,#], Peng Zhang[2,3], Jianxin Deng[5], Jie Liu[5], Francis Fu-Yuen Lam[2], Ronald A Li[6], Yu Huang[2], Jian Jin [1], Xiaoqiang Yao[1,2,3,4*]

[1]School of Medicine and Pharmaceutics, Jiangnan University, Wuxi, China. [2]School of Biomedical Sciences and [3]Shenzhen Research Institute, Chinese University of Hong Kong, China. [4]Department of Physiology, Anhui Medical University, Hefei, China. [5]Department of Pathophysiology, Shenzhen University, Shenzhen, China. [6]Stem Cell and Regenerative Medicine Consortium, University of Hong Kong, Hong Kong

[#], these two authors contribute equally to the work

*, Corresponding author:
Xiaoqiang Yao, Ph.D.
School of Biomedical Sciences
The Chinese University of Hong Kong
Hong Kong, China
Email: yao2068@cuhk.edu.hk

Supplemental Methods

Antibodies and chemicals

Anti-$K_{Ca}2.3$ (APC-025), anti-$K_{Ca}3.1$ (APC-064) and anti-TRPV4 (ACC-034, rabbit) were from Alomone Labs. Anti-TRPV4 (SC-47527, goat) antibody for double immunostaining was from Santa Cruz Biotechnol. Protein A-agarose (product code 11134515001) was from Roche. Fura-2/AM was from Molecular Probes Inc. Alexa Fluor 488 conjugated donkey anti-rabbit IgG and Alexa Fluor 546 conjugated donkey anti-goat IgG were from Invitrogen. 4α-PDD was from Calbiochem. RN1734 was from Menai Organics Ltd. Phenylephrine and acetylcholine were from Sigma. Endothelial cell growth medium (EGM), endothelial cell basal medium (EBM) and bovine brain extract (BBE) were from Lonza Walkersville Inc.

Cell preparation and culture

All animal experiments were conducted in accordance with the regulation of the U.S. National Institute of Health (NIH publication No.8523). Primary mesenteric arterial endothelial cells (MAECs) were isolated from male Sprague-Dawley rats (250-300g) as described elsewhere.[1] Briefly, the abdomen was opened, and the heart was perfused with PBS to remove circulating blood from blood vessels. The small intestine was dissected out and all the vein branches of the mesenteric bed were rapidly excised. The remaining arterial branches were digested with 0.02% collagenase (C9891, Sigma) in EBM for 45 min at 37°C. After centrifugation at 1600×*g* for 5 min, the pelleted cells were resuspended in EGM medium supplemented with 1% BBE, and plated in a flask. Nonadherent cells were removed 1 hr later. The adherent endothelial cells were cultured at 37°C with 5% CO_2 for 3-5 days. These cells were used for experiments without further cell passage. The identity of endothelial cells was verified by immunostaining with an antibody against von Willebrand Factor.

Subcellular localization

Briefly, the freshly isolated rat MAECs were seeded on glass coverslips. After 2 hrs, the cells were rinsed with PBS three times, then fixed with 3.7% formaldehyde and permeabilized with 0.1% Triton X-100. Nonspecific immunostaining was blocked by incubating the cells with 2% BSA in PBS at 23-25°C. Cells were then incubated with a mixture of anti-$K_{Ca}2.3$ (rabbit polyclonal antibody, APC-025) and anti-TRPV4 (goat polyclonal antibody, SC-47527) antibodies per well overnight at 4°C. In some experiments, cells were incubated with a mixture of anti-$K_{Ca}3.1$ (rabbit polyclonal antibody, APC-064) and anti-TRPV4 (goat polyclonal antibody, SC-47527) antibodies per well overnight at 4°C. After three washes with PBS, cells were incubated for 1 hr with a mixture of secondary donkey anti-rabbit IgG conjugated to Alexa Fluor 488 (1:200) and donkey anti-goat IgG-conjugated to Alexa Fluor 546 (1:100) at 23-25°C. After washing and mounting, immunofluorescence of the cells was recorded using Olympus FV1000 Fluoview confocal system. The images were collected in a sequential mode by two different lasers (one argon laser and another HeNe laser) in a confocal microscope. Therefore, cross-over is avoided. The pixel resolution of images was 640 x 640. Furthermore, as a standard control for double immunolabeling studies, control experiments were performed using a single antibody to make sure that there was no cross-over from unwanted fluorescence. All parameters of the confocal system, including laser intensity, gain, aperture, scanning speed, exposure time, microscope lens and magnification, were kept the same in all experiments. In other words, the conditions that we used to detect $K_{Ca}3.1$ and $K_{Ca}2.3$ fluorescence were exactly the same. The observed difference in distribution pattern between $K_{Ca}3.1$ and $K_{Ca}2.3$ ($K_{Ca}3.1$ more cytosolic) could not be attributed to any difference in confocal system parameters. Two Anti-TRPV4 antibodies (SC-47527 from Santa Cruz and ACC-034 from Alomone Labs) had similar subcellular staining pattern when used individually, but only SC-47527 (raised in goat) was suitable for the

double immunolabeling experiments.

Immunostaining of the third order branch of mesenteric arteries

The mesenteric arteries were treated with scrambled-siRNA or TRPV4-siRNA or $K_{Ca}2.3$-siRNA following the method described elsewhere.[2] The arteries were then embedded in OCT compound (4583, Sakura Finetek, the Netherlands), snap frozen and cut into 10 μm thick cryostat sections, then fixed in 4% paraformaldehyde for 30 minutes and treated with 0.05% Triton X in PBS for 1 minute at 23-25^{o}C. The sections were blocked with 5% normal donkey serum for 1 hour at 23-25^{o}C. Primary antibodies against TRPV4 (Alomone Labs) or $K_{Ca}2.3$ were incubated overnight at 4^{o}C. After three washes in PBS, the sections were then incubated with donkey anti-rabbit IgG conjugated to Alaxa Fluor 546 (1:200) or donkey anti-goat IgG-conjugated to Alexa Fluor 546 (1:100) for 1 hour at 23-25^{o}C. The sections were observed under the FV1000 Fluoview confocal system at 23-25^{o}C. Internal elastic lamina displayed relative strong autofluorescence when excited with Argon laser at 488 nm, but only very weak autofluorescence when excited with HeNe laser at 543 nm.

Immunoprecipitation and immunoblots

$K_{Ca}2.3$ or TRPV4 proteins were immunoprecipitated by incubating 800 μg of the extracted proteins with 5 μg of anti-$K_{Ca}2.3$ or anti-TRPV4 (Alomone Labs) antibody on a rocking platform overnight at 4^{o}C. Protein A agarose (11134515001, Roche Applied Science) was then added and incubated for additional 3 hours at 4^{o}C. The immunoprecipitates were washed with saline 3 times and were resolved on an 8% SDS/PAGE gel. For immunoblots, the polyvinylidene difluoride membrane carrying the transferred proteins was incubated with the anti-TRPV4 or anti-$K_{Ca}2.3$ or anti-$K_{Ca}3.1$ primary antibody at a 1:200 dilution. Immunodetection was accomplished using horseradish peroxidase-conjugated secondary antibody, followed by ECL detection system.[3]

Measurement of membrane potentials and $[Ca^{2+}]_i$ using fluorescent dyes

For simultaneous measurement of membrane potentials and $[Ca^{2+}]_i$, the primary cultured MAECs were loaded with 5 μM Fura-2/AM and 100 nM $DiBAC_4(3)$ at 37°C for 10-30 minutes. Fura-2 and $DiBAC_4(3)$ fluorescence signals were measured using an Olympus fluorescence imaging system in cells bathed in a modified Kreb's solution oxygenated with a gas mixture of 95% O_2 and 5% CO_2. The modified Kreb's contained in mM: 119 NaCl, 4.7 KCl, 2.5 $CaCl_2$, 1 $MgCl_2$, 25 $NaHCO_3$, 1.2 KH_2PO_4 and 11 glucose. Fura-2 ratio change (340/380) was then converted to $[Ca^{2+}]_i$ based on the calibration using a calibration kit (Invitrogen). $DiBAC_4(3)$ fluorescence changes were normalized to the fluorescence intensity at the beginning of that experiment (F1/F0). The relationship between $DiBAC_4(3)$ fluorescent intensity and membrane potentials were established previously.[4]

For the measurement of global $[Ca^{2+}]_i$ rise alone, the primary cultured MAECs were loaded with 10 μM Fura-2/AM and 0.02% pluronic F-127 for 10-30 min in dark at 37°C. The cells were bathed in the modified Kreb's solution oxygenated with a gas mixture of 95% O_2 and 5% CO_2. Fura-2 fluorescence signals were measured at room temperature using dual excitation wavelengths at 340 and 380 nm using an Olympus fluorescence imaging system.

Confocal line-scan imaging method was used to measure local $[Ca^{2+}]_i$ rises. The primary cultured MAECs were loaded with Fluo-4 AM (5 μM, 10 min) for detecting the localized Ca^{2+} activity/spike-like signals. Confocal line-scan imaging was performed at 488 nm excitation and 505 nm collection with a 63× oil immersion lens. Line-scan images were acquired at sampling rate of 3.84 ms per line, along with the longitudinal axis of the cell. If needed, endothelial cells were challenged with acetylcholine (ACh, 1 μM) or 4α-PDD (5 μM).

Membrane potential measurement using whole-cell patch clamp

An EPC-9 patch clamp amplifier was used to measure the membrane potentials of cultured MAECs in whole-cell perforated patch mode. The pipette solution contained (in mM): 105 K^+-gluconate, 30 KCl, 1 $MgCl_2$, 10 NaCl, 10 HEPES, pH 7.2, with 250 μg/ml amphotericin. Bath solution was NPSS, which contained in mM: 140 NaCl, 5 KCl, 1 $CaCl_2$, 1 $MgCl_2$, 10 glucose, 5 HEPES, pH 7.4. When needed, 4α-PDD or acetylcholine was applied to the bath solution.

Membrane potential measurement of smooth muscle cells in arterial segments using sharp microelectrodes

Segments of rat mesenteric arteries were dissected into ~3 mm rings. The arterial segments were opened longitudinally and equilibrated for 60 min in Kreb's solution oxygenated with a gas mixture of 95% O_2 and 5% CO_2. Membrane potentials were measured using glass microelectrodes filled with 3 M KCl (resistance: 40-60 MΩ). Electrodes were inserted into smooth muscle cells from adventitial side. Successful impalement was indicated by an abrupt drop in voltage, followed by a sharp return to baseline on exit. Electrical signals were monitored continuously by an EPC9 amplifier (HEKA) with Pulse software.

Arterial tension measurement

2 mm segments of the third- or fourth- branches of rat mesenteric arteries were mounted in a DMT myograph (model 610M, Danish Myo Technology, Aarhus, Denmark) and changes in isometric tension of arteries were measured. The rings were stretched to an optimal baseline force of 2 mN for 2 mm artery segments. The force and wall tension relationship is defined by tension = force/2 x segment length. The optimal force is equivalent to that generated at 0.9 times the diameter of the vessel at 100 mmHg.[5] Artery segments were pre-contracted with phenylephrine. The concentration of phenylephrine varied from 3 to 10 μM to achieve similar degree of constriction in different arteries. Agonists were added in a cumulative fashion to the bath to obtain concentration-response curves. The bath solution is the modified Kreb's solution.

Simultaneous measurement of blood pressure and blood flow in mesenteric vascular beds in live rats

SD rats (280-320 g) were anaesthetized with ketamine (35 mg kg^{-1}) plus xylazine (7 mg kg^{-1}). After performing a midline laparotomy, ~2/3 of rat mesenteric arterial bed was softly put into a petri-dish chamber and bathed in Kreb's solution. Blood perfusion of rat mesenteric arterial bed was assessed with a Laser Doppler perfusion imager (amoorFLPI full-field image, Moor Instruments, Devon, UK). The acquisition was made in high resolution mode with 5 s interval. The pixel resolution of images was 760 x 568. The digital color-coded images were analyzed to quantify blood flow in the region from mesenteric vascular beds. Blood pressure of the rats was simultaneously monitored through pressure transducer inserted in common carotid artery. When needed, the bathing solution was changed to the one's containing 4 μM 4α-PDD or 1 μM acetylcholine.

siRNA transfection

MAECs were transfected with TRPV4-siRNA, K_{Ca}2.3-siRNA or a scrambled-siRNA as control by electroporation using Nucleofector II (ADD-1001s, Amaxa biosystems) following the procedure in manufacturer's instruction manual. About 70% of MAECs were successfully transfected by respective protocols as indicated by control transfection using a GFP-expressing pCAGGS vector. Functional studies were performed 2-3 days post-transfection.

Third order of rat mesenteric arteries were transfected using Lipofectamine RNA_imax (133778-075, Invitrogen).[2] Briefly, arteries were incubated for 24 hours (37°C, 5% CO_2) in a mixture of 100 nM TRPV4-siRNA or K_{Ca}2.3-siRNA and 5 μl of Lipofectamine RNA_imax in DMEM. Subsequently, complete medium was added and arteries were left another 48 hours before being used in myograph or electrophysiology. For the control, acetylcholine-induced relaxation in mesenteric arteries was not altered by the siRNA transfection procedure, suggesting that the procedure did not affect the integrity of endothelial cell function in these arteries (Figure S12).

Induction of diabetes

SD rats (250-280g) received 0.1 M citrate buffer or a single dose of streptozotocin (60 mg/kg, i.p.). About 72 h after streptozotocin treatment, fasting glucose levels in blood taken from the tail vein early in the morning were measured using a commercial glucometer (Ascensia ELITE®, Bayer, IN). Rats with glucose levels >15 mM were considered diabetic. After the onset of diabetes, 12-15 weeks after streptozotocin or vehicle treatment, the rats were killed for studies.

Statistics

Paired two tailed Student's t-test was used for two group comparison in Figure S4, S6 and S11. One-way ANOVA with Newman-keuls was used in Figure S1C and S3. Two-way ANOVA followed by Bonferroni post-test was used for comparison of multiple groups in Figure S9 and S10 (GraphPad). For dose response curves (Figure S1D, S7, S8 and S12), acetylcholine or 4α-PDD concentration was transformed into Log values and the data were fitted with sigmoidal dose-response curves. F-test was performed to compare the best-fit values of E_{MAX} and EC_{50} between different treatments (GraphPad). $p<0.05$ was considered as significant different.

Supplemental References:

1. Ashley RA, Dubuque SH, Dvorak B, Woodward SS, Williams SK, Kling PJ. Erythropoietin stimulates vasculogenesis in neonatal rat mesenteric microvascular endothelial cells. *Pediatr Res.* 2002; 51: 472-478.
2. Sharif-Naeini R, Folgering JH, Bichet D, Duprat F, Lauritzen I, Arhatte M, Jodar M, Dedman A, Chatelain FC, Schulte U, Retailleau K, Loufrani L, Patel A, Sachs F, Delmas P, Peters DJ, Honoré E. Polycystin-1 and -2 dosage regulates pressure sensing. *Cell*. 2009; 139: 587-596.
3. Ma X, Qiu S, Luo J, Ma Y, Ngai CY, Shen B, Wong CO, Huang Y, Yao X. Functional role of vanilloid transient receptor potential 4-canonical transient receptor potential 1 complex in flow-induced Ca^{2+} influx. *Arterioscler Thromb Vasc Biol.* 2010; 30: 851-858.
4. Kwan HY, Shen B, Ma X, Kwok YC, Huang Y, Man YB, Yu S, Yao X. TRPC1 associates with BK_{Ca} channel to form a signal complex in vascular smooth muscle cells. *Circ Res.* 2009; 104: 670-678.
5. Mulvany MJ, Halpern W. Contractile properties of small arterial resistance vessels in spontaneously hypertensive and normotensive rats. *Circ Res.* 1977; 41: 19–26.

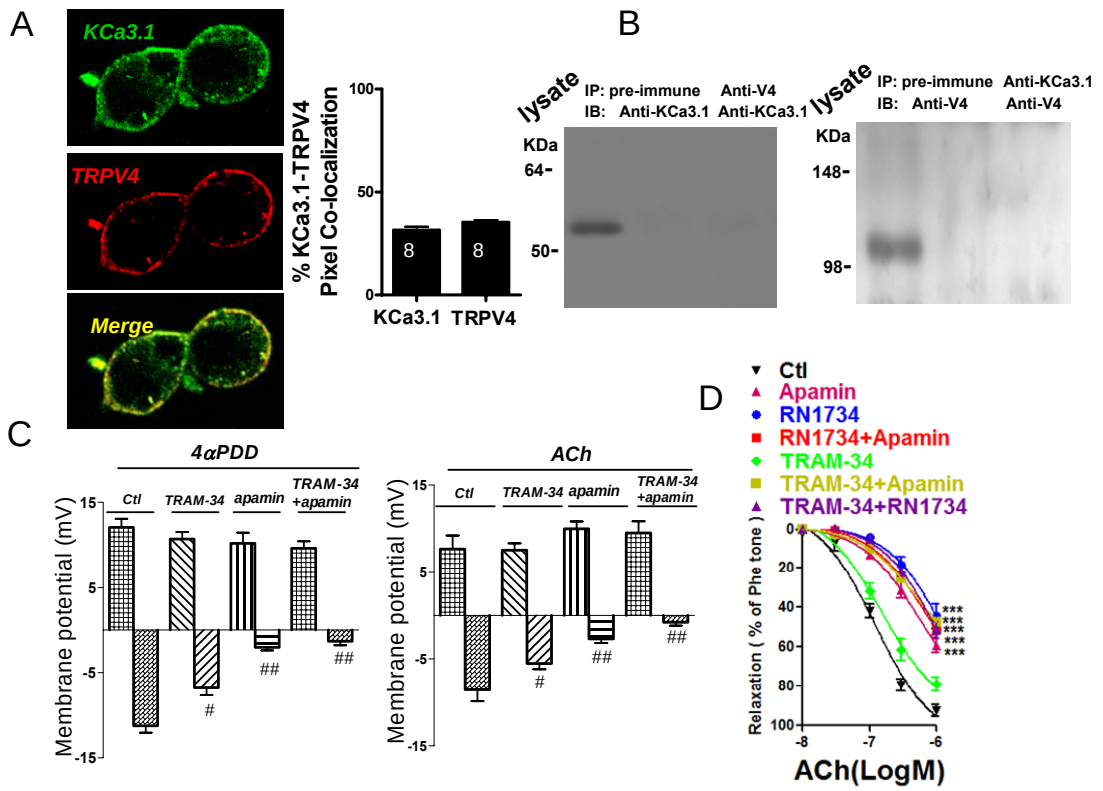

Figure S1. Physical and functional coupling of TRPV4 and $K_{Ca}3.1$ in the primary cultured rat MAECs. **A**, Subcellular co-localization of TRPV4 with $K_{Ca}3.1$ in the primary cultured rat MAECs. Shown were immunostaining images of $K_{Ca}3.1$ (green) and TRPV4 (red) in two representative cells; Also shown were the overlay image (merge) and data summary illustrating the percentage of TRPV4-$K_{Ca}3.1$ pixel co-localization (right, n = 8 cells). **B**, Co-immunoprecipitation in the primary cultured rat MAECs. The pulling antibody and blotting antibody were indicated. Control immunoprecipitation was done using the preimmune IgG (pre-immune). IP, immunoprecipitation; IB, immunoblot; anti-V4, anti-TRPV4. *n* = 3 experiments. **C**, Summary data of perforated patch clamp studies showing the effect of $K_{Ca}3.1$ and/or $K_{Ca}2.3$ inhibition on 4α-PDD (5 μM)-induced and acetylcholine (ACh, 1 μM)-induced biphasic changes in membrane potentials. If needed, MAECs were pretreated with TRAM-34 (1 μM) or apamin (200 nM) for 30 min. Data are shown as mean ± S.E. *n* = 3-5 experiments. One-way ANOVA with Newman-keuls post hoc test was used to compare the difference between groups. $P<0.05$ compared to control; ##, $P<0.01$ compared to controls. **D**, Summary data of myograph studies showing the effect of TRPV4 and/or $K_{Ca}3.1$ and/or $K_{Ca}2.3$ inhibition on acetylcholine-induced relaxation. Data in mean ± S.E were fitted with sigmoidal dose response curve. F-test was used to compare the best-fit values of E_{MAX} and EC_{50} between different groups. *n* = 3-4 experiments. ***, $P<0.001$ compared to control (Ctl) for EC_{50}.

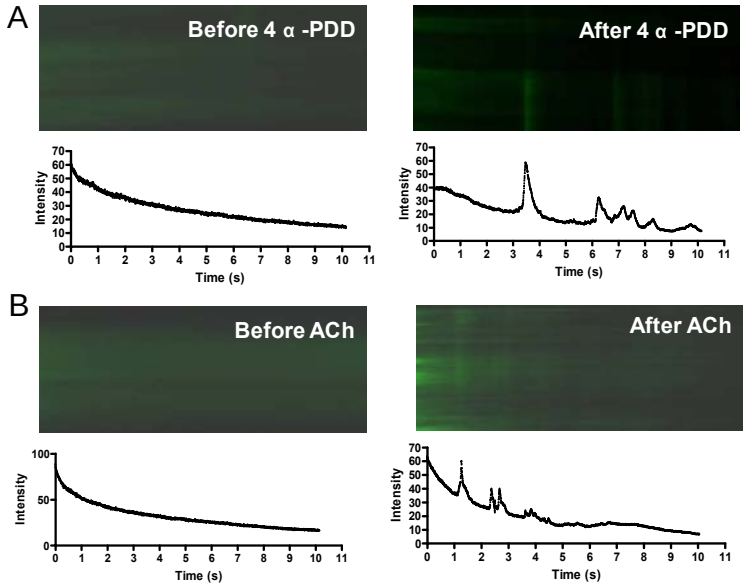

Figure S2. 4α-PDD- and acetylcholine-induced local Ca^{2+} signals in rat MAECs. **A and B**, Representative Ca^{2+} images (upper panel of **A and B**) and traces (lower panel of **A and B**) showing changes in the activity of local Ca^{2+} signals before and after bath application of 4α-PDD (5 μM) and acetylcholine (ACh, 3 μM). MAECs were loaded with Fluo-4/AM (5 μM, 10 min). Line-scan images were acquired at sampling rate of 3.84 ms per line, along with the longitudinal axis of the cell. *n* = 6-11 experiments.

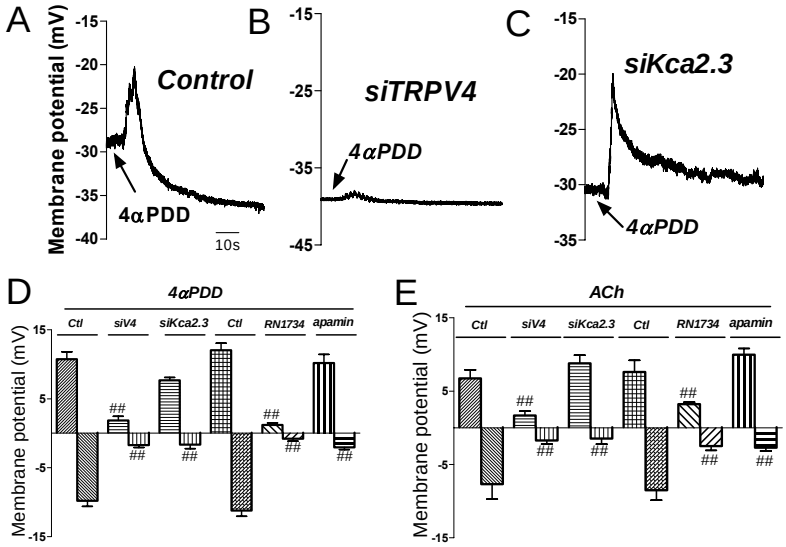

Figure S3. Effect of TRPV4 or $K_{Ca}2.3$ inhibition on 4α-PDD-induced and acetylcholine-induced biphasic changes in endothelial cell membrane potentials. Membrane potentials were measured by perforated patch clamp technique. Shown were representative traces (**A-C**) and summary data (**D-E**). The maximal level of depolarization and hyperpolarization was plotted in D and E. 4α-PDD (5 μM, **A-D**); acetylcholine (ACh, 1 μM, **E**). If needed, MAECs were pretreated with RN1734 (10 μM) or apamin (200 nM) for 30 min, or transfected with siRNAs. Data are shown as mean ± S.E. *n* = 3-8 experiments. One-way ANOVA with Newman-keuls post hoc test was used to compare the difference between groups. ##, $P<0.01$ compared to respective controls.

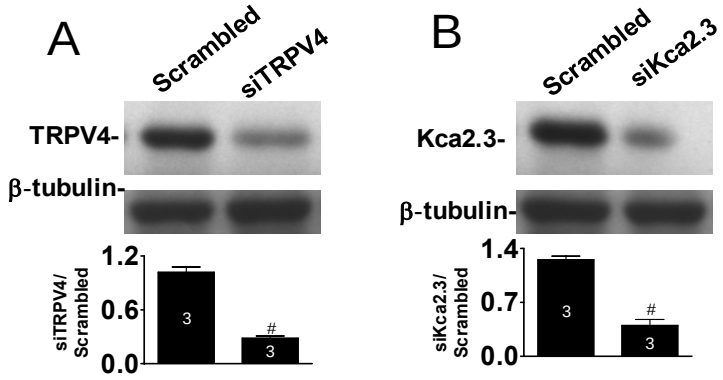

Figure S4. Effectiveness of TRPV4-siRNA and K_{Ca}2.3-siRNA in suppressing the expression of their targeted proteins in rat primary cultured MAECs. **A**, TRPV4-siRNA; **B**, K_{Ca}2.3-siRNA. Shown are representative images (upper) and data summary (lower) of immunoblot experiments. Scrambled siRNA had no effect. Immunoblots with anti-β-tubulin antibody showed that equal amounts of protein were loaded onto each lane. Data are shown as mean ± S.E. *n* = 3 experiments. Paired two tailed Student's t-test was used to compare the difference between two groups. #, $P<0.01$ compared to scrambled controls.

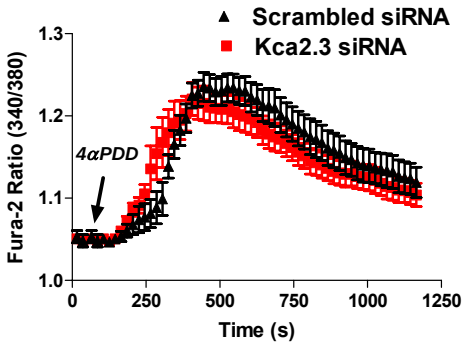

Figure S5. Lack of K_{Ca}2.3-siRNA effect on 4α-PDD-induced $[Ca^{2+}]_i$ rises in rat MAECs. Cells transfected with scrambled siRNA were used as control. 4α-PDD, 5 μM. Data are shown as mean ± S.E. *n* = 3-4 experiments.

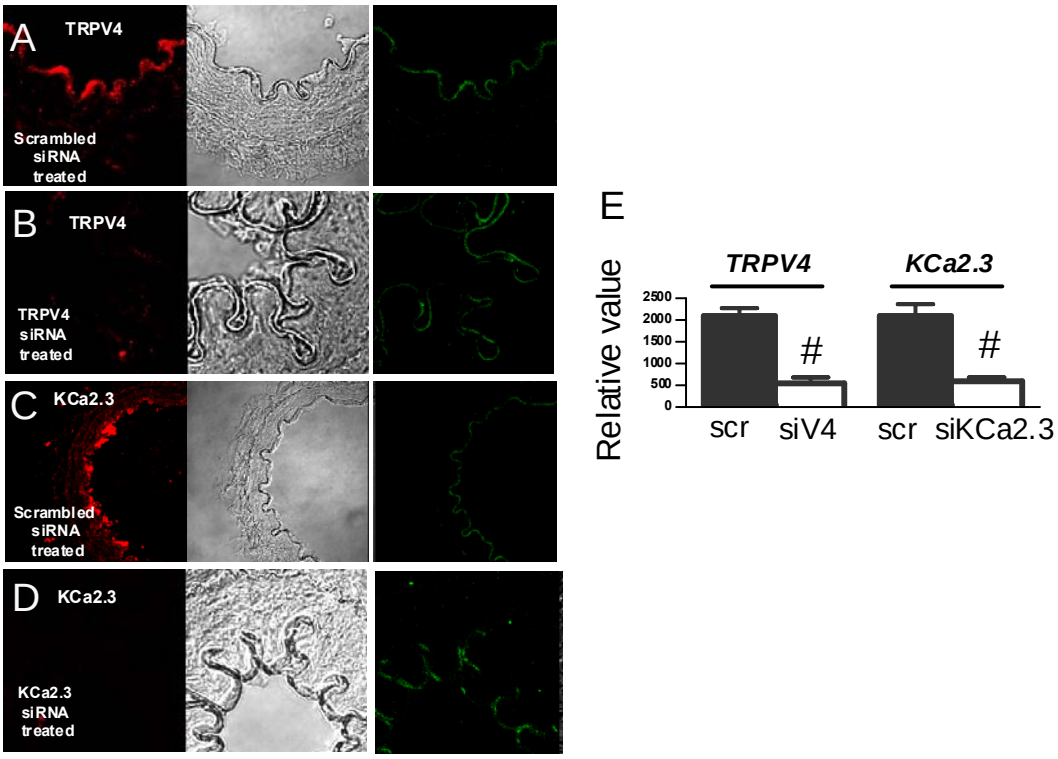

Figure S6. Effect of TRPV4-siRNA and K_{Ca}2.3-siRNA on the expression of TRPV4 and K_{Ca}2.3 proteins in the endothelial cells of the third-order mesenteric arteries. Shown were representative images (**A-D**) and summary data (**E**) of TRPV4 expression (**A**), TRPV4-siRNA effect (**B**), K_{Ca}2.3 expression (**C**), and K_{Ca}2.3-siRNA effect (**D**) in the third-order mesenteric arteries. Left, immunostaining images using anti-TRPV4 (**A-B**) and anti-K_{Ca}2.3 (**C-D**) antibodies; middle, corresponding bright-field images; right, autofluorescence of internal elastin lamina underneath the endothelium (excitation: 488 nm, Green). Scrambled siRNA (scr) was used as control. Note that TRPV4-siRNA and K_{Ca}2.3-siRNA treatment apparently had no effect on green signals (autofluorescence from internal elastic lamina), but drastically reduced the red signals (from TRPV4 and K_{Ca}2.3 staining). Data are shown as mean ± S.E. n = 4-8 experiments. Paired two tailed Student's t-test was used to compare the difference between two groups. #, P<0.05 compared to control.

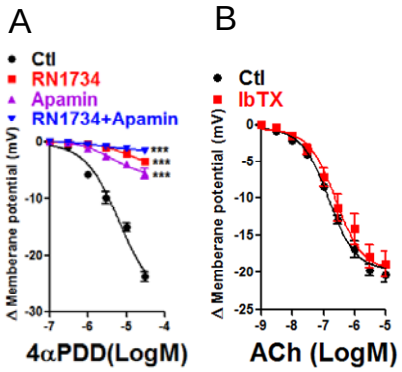

Figure S7. Effect of RN1734, apamin and iberiotoxin on 4α-PDD or acetylcholine-induced hyperpolarization of smooth muscle in isolated mesenteric artery strips. Membrane potentials were measured by sharp microelectrodes impaled from adventitial side. A, 4α-PDD (0.3-30 μM). B, ACh (3 nM-10 μM). If needed, arterial strips were pretreated with RN1734 (10 μM, A) or apamin (200 nM, A) or iberiotoxin (IbTX, 100 nM, B) for 30 min. Data in mean ± S.E were fitted with sigmoidal dose response curve. F-test was used to compare the best-fit values of E_{MAX} and EC_{50} between different groups. *n* = 4-8 experiments. ***, *P*<0.001 compared to control for E_{MAX} and EC_{50}.

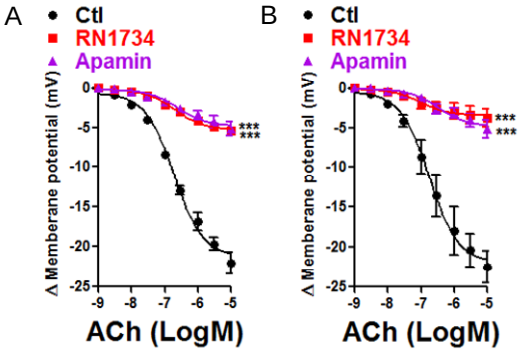

Figure S8. Comparison of acetylcholine-induced smooth muscle cell hyperpolarization using two different methods. **A,** Artery segments were opened longitudinally. Sharp microelectrodes were impaled from adventitial side. **B,** Artery segments were mounted in wire myographs, and the sharp microelectrodes were impaled from adventitial side. Acetylcholine, 3 nM-10 μM. If needed, arterial segments were pretreated with RN1734 (10 μM) or apamin (200 nM) for 30 min. Data in mean ± S.E were fitted with sigmoidal dose response curve. F-test was used to compare the best-fit values of E_{MAX} and EC_{50} between different groups. *n* = 3-4 experiments. ***, *P*<0.001 compared to control for both E_{MAX} and EC_{50}.

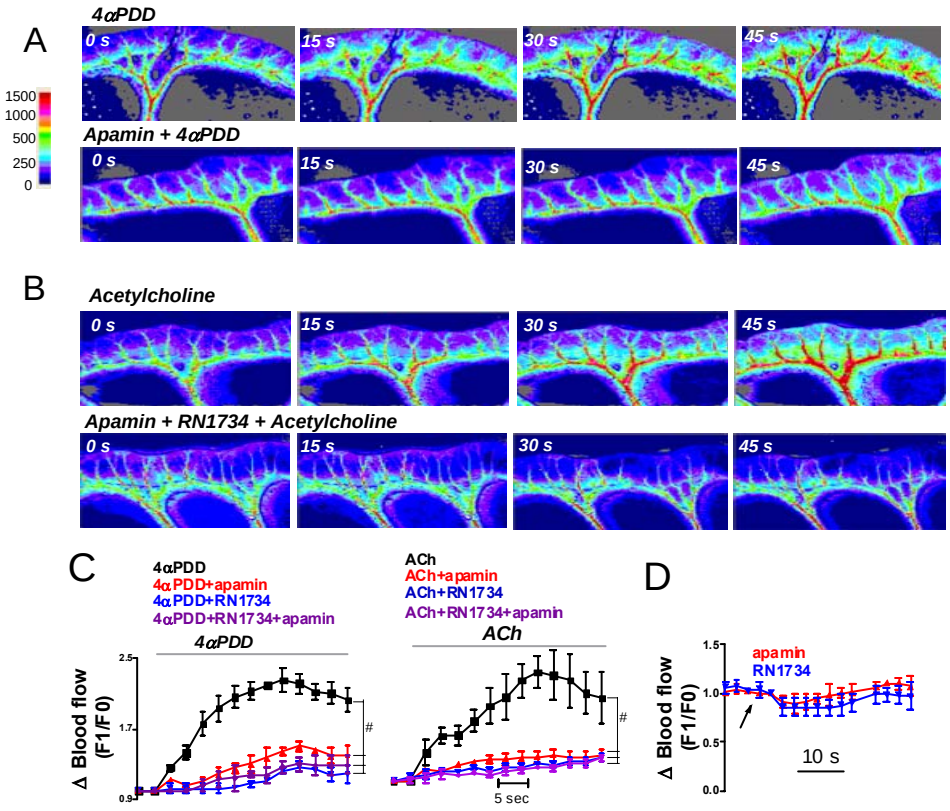

Figure S9. Role of TRPV4-K_{Ca}2.3 pathway in the control of local blood flow in mesenteric bed *ex vivo*. **A and B:** Representative images of Laser Doppler studies illustrating 4α-PDD (4 μM, **A**) and acetylcholine (1 μM, **B**)-elicited increase in blood perfusion in the mesenteric arteries from the forth-order to the end. The lower panel in A and **B** showed the effect of apamin (200 nM) or RN-1734 plus apamin (10 μM and 200 nM, respectively). The color scale bar quantifies the blood perfusion, with red being the highest and dark blue being the lowest. **C,** Summary data of Laser Doppler studies as in **A** and **B**. Data are shown as mean ± S.E. *n* = 4-8 experiments. Two-way ANOVA followed by Bonferroni post-test was used to compare the difference. #, $P<0.001$ compared to control. **D**, Effect of inhibitors alone on blood flow. RN1734 (10 μM, blue) or Apamin (200 nM, red). Data are shown as mean ± S.E. *n* = 4-8 experiments.

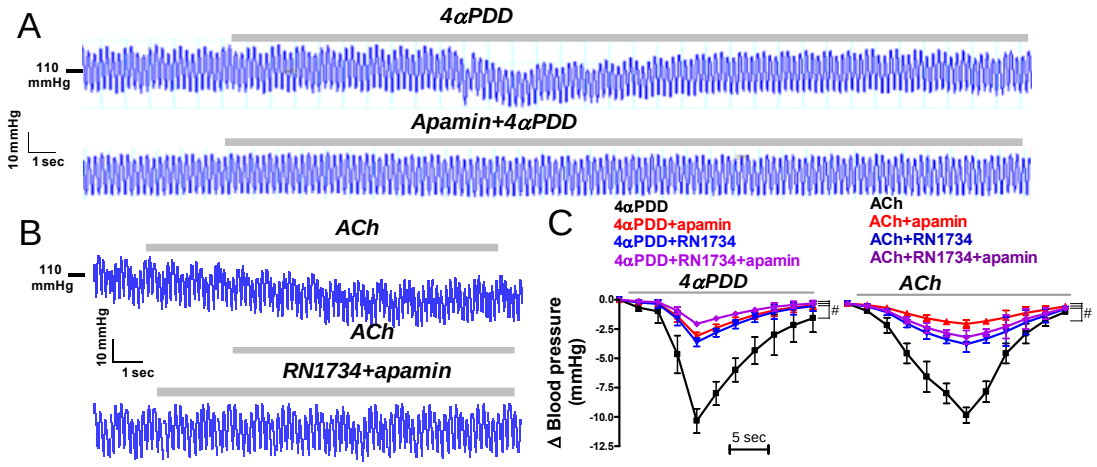

Figure S10. Role of TRPV4-K_{Ca}2.3 pathway in the control of systemic blood pressure. **A-B**, representative traces of blood pressure change illustrating 4α-PDD (4 μM, **A**)- and acetylcholine (1 μM, **B**)-elicited decrease in blood pressure. Lower traces in A and B showed the effect of apamin (200 nM, **A**) and RN1734 plus apamin (10 μM and 200 nM, respectively, **B**). **C**, Summary data of blood pressure measurement. Data are shown as mean ± S.E. n = 4-8 experiments. Two-way ANOVA followed by Bonferroni post-test was used to compare the difference. #, P<0.001 compared to control. #, P<0.05 compared to control.

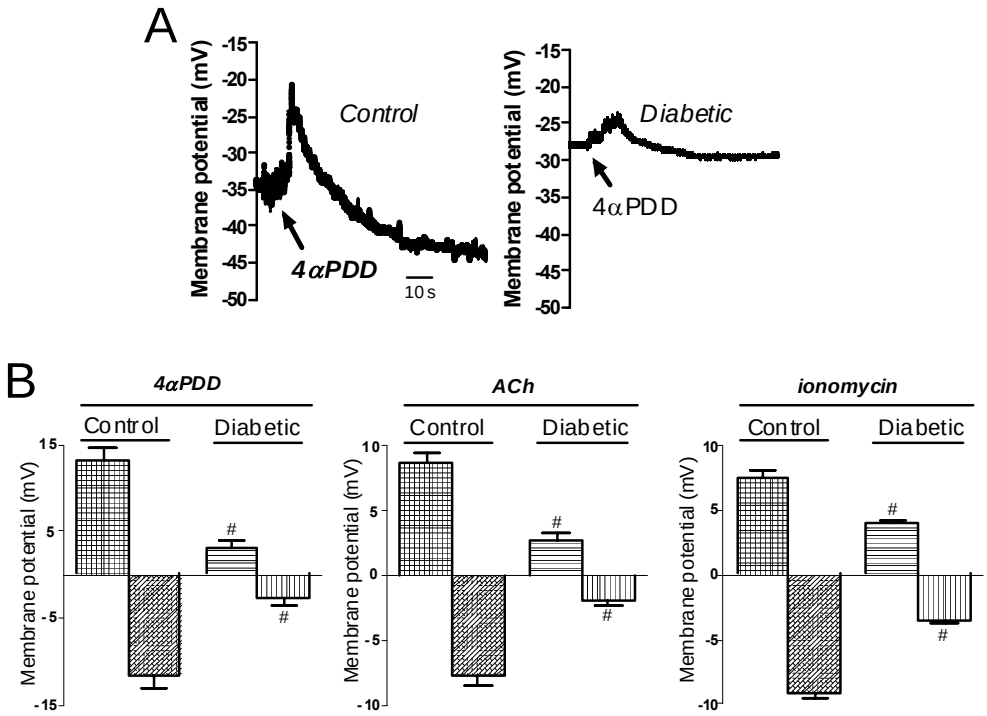

Figure S11. 4α-PDD-induced, acetylcholine-induced and ionomycin-induced biphasic changes in endothelial cell membrane potentials between normal and diabetic rats. Membrane potentials in rat MAECs were measured by perforated patch clamp technique. Shown were representative traces (**A**) and summary data (**B**). 4α-PDD (5 μM, **A** and **B**); Acetylcholine (ACh, 1 μM, middle in **B**); Ionomycin (3 μM, right in **B**). Control, normal rats. Data are shown as mean ± S.E. n = 4-8 experiments. Paired two tailed Student's t-test was used to compare the difference between two groups. #, P<0.05 compared to control.

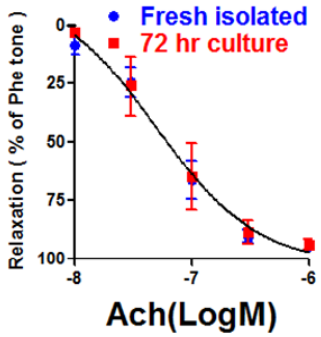

Figure S12. Effect of culturing rat mesenteric artery segments *in vitro* for 72 hr on acetylcholine-induced vascular relaxation. Acetylcholine-induced vascular relaxation of rat small mesenteric artery segments was measured by wire myograph. Data are shown as mean ± S.E. n = 3-4 experiments. Data in mean ± S.E were fitted with sigmoidal dose response curve. F-test was used to compare the best-fit values of E_{MAX} and EC_{50} between different groups. No significant difference was found between two groups.